https://doi/org/10.5281/zenodo.5228497

Signature of 3600-yr LaViolette flare in Antarctica ^{10}Be spectra

Mensur Omerbashich
https://orcid.org/0000-0003-1823-4721, editor@geophysicsjournal.com

Abstract. ^{10}Be deposition rates from Vostok, Antarctica raw ice core records are periodic with 3592±57 yr at 99% significance, verified against the ^{10}Be concentration raw data from both Vostok, as 3700±57 yr at 99%, and Taylor Dome, Antarctica, as 3800±61 yr at 99%. Also, Mg concentration data from Taylor Dome cycle every 3965±16 yr at 99%. The Vostok data respond to the Hallstadzeit Solar cycle, as 2296±57 yr at 99%, perhaps its best estimate yet. After data separation at $2 \cdot 10^5$ atoms/cm^2/yr (deposition rates) and $0.95 \cdot 10^5$ atoms/g of ice (concentrations) cutoffs, reflecting cosmic-ray background conditions at the Galactic boundary, only the discovered period remains and converges, as 3378±103 yr and 3346±85 yr, respectively; the Hallstadzeit cycle vanishes in both cases. Thus the observed ~3600-yr period is of extrasolar but galactic origin. Since ^{10}Be periodicity is explainable only by rapid excesses in the atmospheric cosmic-ray influx, the discovered period is the signature of a regular burst occurrence from a galactic source. Based on 500-parsec Galactic Center (GC) GeV/TeV γ-ray surveys by the H.E.S.S. and INTEGRAL telescopes, the GC's extremely active central region makes the best candidate-host for such bursts recently observed by ROSAT and Fermi satellites. I estimate the most recent epoch of ^{10}Be maximum as 1085±57 CE, coinciding with the 1054–1056 CE historical account apparently of SN1054 (Crab supernova), and predict the next maximum ^{10}Be in 4463±57 CE. Given continuous decadeslong exposure and the relatively short return period coinciding with known cataclysms, this recurrent LaViolette flare affects the Earth climate significantly.

Beryllium analysis; Vostok ice cores; cosmic rays; paleoclimate; Hallstadzeit cycle; LaViolette flares.

---

1. Introduction

Since climate variations largely recur, climate research relies greatly on spectral analyses for paleoclimate studies and modeling. Orbital, solar, and galactic processes are the most explored sources of periodic variations of climate. Bard and Frank (2006) give a good overview of research on the Sun radiation as the main suspect for significant changes in Earth climate.

Usually, records of various proxies are used for making inferences on past atmospheric conditions. For instance, it is held commonly that the relatively stable radioactive isotope Beryllium 10 (^{10}Be) with a half-life of 1.6 million years (myr) is cosmogenic, i.e., created by irradiation when cosmic rays (carbon, nitrogen, oxygen, and other nuclei, i.e., particles charged with very high energy, 100GeV to 10^{15} eV) collide with helium and hydrogen ions as the rays travel through Space. Thus ^{10}Be is believed not to have been created together with most of the Universe matter, which could explain why ^{10}Be *in situ* concentrations are minute. Hence, ^{10}Be found on Earth is thought to mostly come from the atmospheric fallout, where the ^{10}Be atoms are made by cosmic rays colliding with the atmospheric nuclei. The atoms are subsequently transported in snowflakes from the atmosphere onto the Earth's surface, where they become part of ice sheets by adhering to suspended particles in the water column or the sedimentary record by adsorbing onto available clay particles. So captured, ^{10}Be atoms are invaluable as a dating proxy in climate studies in which the counting of captured atoms helps detect causes to a differential influx of the cosmic ray radiation; the Sun strength is one such candidate cause.

The cosmic rays could be responsible for Earth climatic disturbances because cosmic rays make up a significant portion of the energy density of the interstellar medium (Longair, 2002). Many theoretical studies of galactic sources of the cosmic rays have been undertaken since LaViolette (1983, 1987) first proposed Galactic Centre (GC) explosions as a cause for climatic changes on Earth. The related observational studies of TeV γ-ray sources in our galaxy have gained an impetus over the last few years with the low-energy-threshold (100 GeV) H.E.S.S. telescope array (Benbow, 2005, Aharonian *et al.*, 2006, 2005), the INTEGRAL telescope array (Bélanger, 2006) and other telescope GeV/TeV γ-ray surveys of the central 500-parsec region of GC. GC is interesting for such studies as it is the most unusual part of our galaxy (Morris and Serabyn, 1996). One of the achievements of the ground-based γ-ray astronomy since its inception in 2002 is the recognition of GC as a TeV γ-ray source (Hofmann, 2005), with more than 30 γ-ray sources detected so far using H.E.S.S. telescope (Benbow, 2006). One of the most favored models for galactic sources of high-energy cosmic rays has been the diffusive shock acceleration in supernova remnants (SNR), e.g., Aharonian (2004). However, there are serious issues even with that model (Hillas, 2005), such as the detection of a supernova SN 1006 emitting no significant γ-rays over its entire field of view, as well as a possibility of a new class of cosmic accelerators perhaps driven by shock winds of massive objects emitting TeV energy (Hofmann, 2005). Recently, Bland-Hawthorn et al. (2019) reported evidence from ROSAT and Fermi satellites of a Milky Way GC explosion several myr ago, resembling GC explosions seen in Seyfert-type galaxies.

Climate studies face intricate problems in understanding ice core data such as ^{10}Be properly. A notable contributor to the error budget is the reliability of the timescales used. The introduction of an excess of dating methods (and consequently numerous timescales) into climate studies has led Monnin *et al*. (2004) to question the whole dating approach. The main problem with present methodologies in climate science is in a common approach to data treatment and spectral analysis: "let us prepare data so that data satisfy limited abilities of the classically used Fourier spectral analysis (FSA) and its derivative methods". Drawbacks of classical approaches – such as the need to boost signal in very long records – require severe data alterations. For example, researchers often invent data to make their analyzed records equispaced; the requirement for equispaced time-series being the main disadvantage of the Fourier-derived methods. Sometimes even approaches to data handling and preparation are accommodated to the processing algorithms at hand. It is remarkable how easy it is for many researchers nowadays to decide pro damaging the nature-given strength of data. In that way, many of the unknown yet intrinsic data relationships and distributions unavoidably get altered. This data alteration is one of the most pressing issues of modern science. As a consequence, researchers more and more rely on ever-complex algorithms. The data alteration problem has caused observational physical sciences to diverge from modeling nature to instead modeling human errors in understanding nature.

Quite oppositely, I regard the use of raw (gapped and unaltered such as by padding, filtering, tapering, and windowing) data as *the* criterion for the validity of a physical result. Interestingly, I was able to show that climate studies desire such a new philosophy to data treatment and analysis, demonstrated to be useful for science in general (Omerbashich, 2006). This perfectly natural approach that regards raw data as the key criterion for the validity of a physical claim can hopefully be welcome by climate researchers forced to work with so many polluted and unreliable data records, with time scales so plentiful yet remarkably inconsistent. For example, each time scale sets its initial stage for new inconsistencies in the spectral analysis. Such discrepancies only add to the unreliability of the spectra that are *a priori* affected by drawbacks of the Fourier spectral analyses (FSA) as the most used spectral analysis method across disciplines. This unsuitability of the FSA is particularly true for long gapped records (Press *et al*., 2003), such as most records of natural data. As a result of this (virtually) chaotic situation in science in general, numerous climate studies range in their conclusions wildly, from one extreme ("*it's the humans!*") to another ("*it's Milankovitch!*") to offbeat speculation ("*it's galactic!*").

2. Data

Due to its remoteness and extreme climate, the most reliable and consistent records of ^{10}Be data found naturally anywhere in the world are those extracted from Antarctica ice cores, Fig. 1. Vostok is Antarctica's first scientific station. Located at S78º 28' E106º 48', it became operational on 16 December 1957. The ice sheet thickness at Vostok is around 3700 m. The Byrd and Taylor Dome polar stations lay both within some 2000 km from Vostok. I use the Vostok ^{10}Be data as my reference data.

https://doi/org/10.5281/zenodo.5228497

Cosmogenic radionuclides (such as ^{10}Be and ^{14}C) records are the most reliable proxies to extend solar activity reconstructions beyond the direct observations of the Sun. High solar shielding of the galactic cosmic rays during periods of high solar activity supposedly decreases the radionuclide production rates and vice-versa for low solar activities. The geomagnetic field also influences cosmogenic radionuclide production rates. Similar to the solar magnetic modulation, the high geomagnetic field intensity is believed to reduce the flux of galactic cosmic rays and radionuclide production rates and vice-versa for low geomagnetic field intensity.

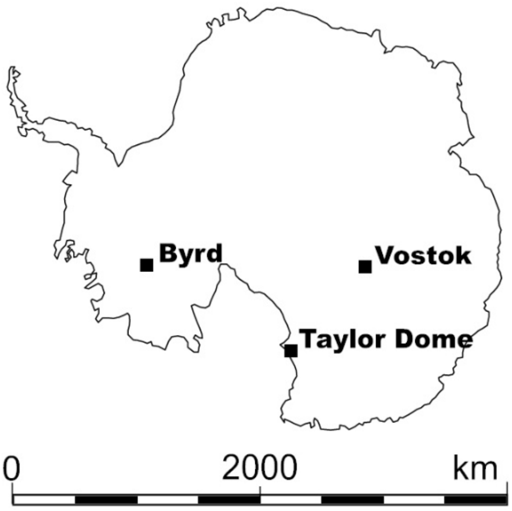

Figure 1. Antarctica: location of world's most reliable ^{10}Be ice core data.

The processes responsible for radionuclide production are well known and can be modeled quantitatively. The highest uncertainties lie in the interpretation of the radionuclide records that can be measured in natural archives such as ice cores in the case of ^{10}Be or tree rings in the case of ^{14}C. This is because changes in atmospheric transport and deposition in the case of ^{10}Be or changes in the carbon cycle in the case of ^{14}C can influence the measured concentrations. Unidentified climatic influences lead to errors in the reconstruction of solar activity changes based on these records. This problem is illustrated by two alternative reconstructions of past changes in solar activity based on ice core ^{10}Be records. Based on a ^{10}Be record from Antarctica Bard *et al*. (2000) conclude that current levels of solar activity were also reached or exceeded around 1200 CE. By contrast, Solanki *et al*. (2004) concluded that solar activity during recent decades is exceptionally high compared to the past 8000 years. The latter authors' method seems to be confirmed by a ^{10}Be record from Southern Greenland, Dye 3 ice core (Beer *et al*., 1990). However, the two ^{10}Be records from Antarctica and Greenland exhibit substantial disagreements for the last 55 years, which is the main reason for these very different conclusions (Raisbeck and Yiou, 2004).

Assuredly, at least one of these records must be influenced by changes in climate as well. Since different geochemical behaviors affect ^{14}C and ^{10}Be, an investigation of ^{14}C records can help solve the contradictions. And because carbon cycle models allow us to understand past changes in atmospheric CO_2 and ^{13}C concentrations, it is also possible to use these models and infer the ^{14}C production rate based on measured ^{14}C concentrations in tree rings. Until 1950 CE, when significant amounts of anthropogenic ^{14}C were released into the atmosphere by the nuclear weapons tests, we can calculate the variations in the ^{14}C production rates and infer the solar magnetic modulation from these records. There are uncertainties in connecting the ^{14}C production rate to recent instrumental measurements of solar magnetic modulation. However, regardless of these uncertainties, the conclusions by Usoskin *et al*. (2003) and Solanki *et al*. (2004) cannot be confirmed by the analysis of the ^{14}C records (Muscheler *et al*., 2005). The ^{14}C tree ring records indicate that today's solar activity is high but not exceptional during the last 1000 years.

https://doi/org/10.5281/zenodo.5228497

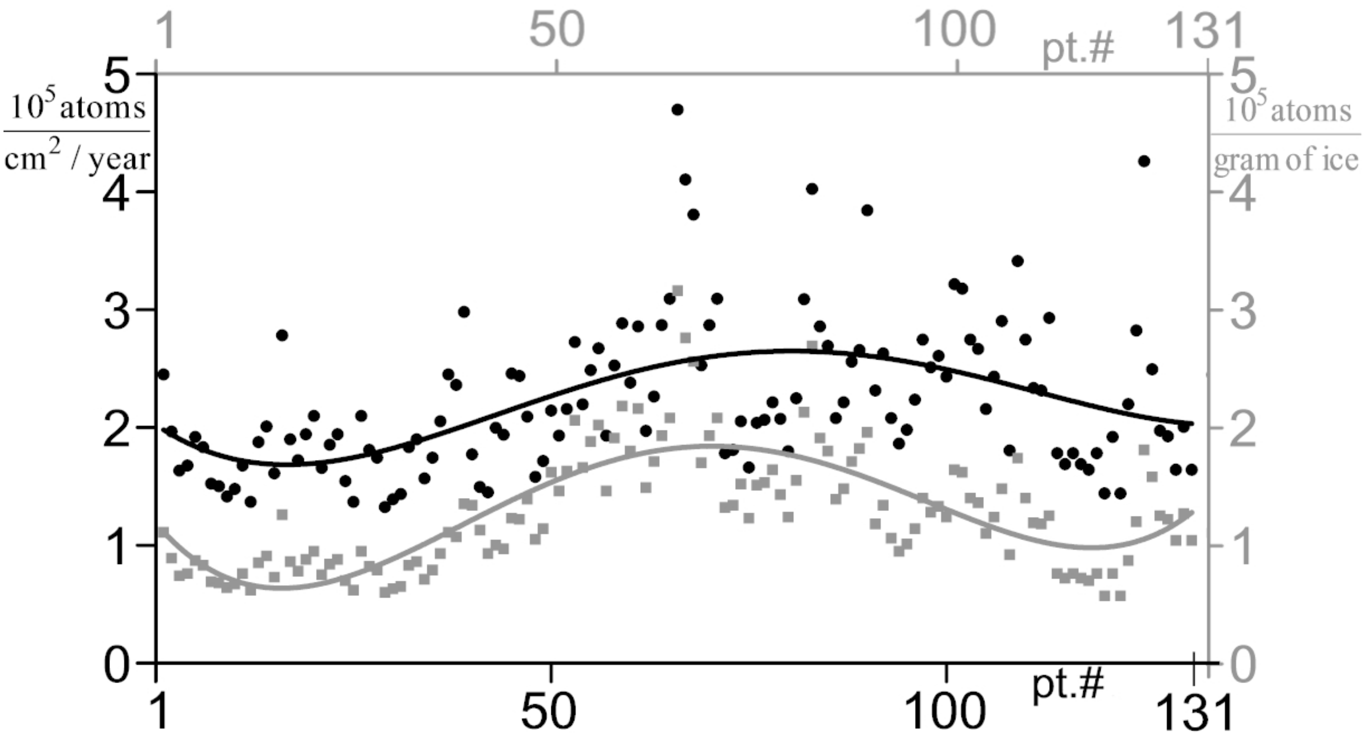

Figure 2. Plot of values, Table 1, of ^{10}Be data at Vostok (Raisbeck *et al*., 1987, 1992): deposition rates (black) v. concentrations (gray). To depict the raw data' cyclic tendency, shown is 4th order polynomial fit as a trend over uniformly distributed values (131 dataset points). Note that here, since we operate in the domain of the raw-data criterion, it is deemed absurd to employ time-plots of raw (gapped) data.

As discussed above, I regard Vostok data as the most reliable of all ^{10}Be ice core datasets. I use for verification purposes different paleoenvironmental data with varying timescales and methodologies in data preparation. So, the data used in this study were ^{10}Be data (both deposition rate and concentration) from Antarctica stations at Vostok (Raisbeck *et al*., 1987, 1992) with LaViolette (1983) timescale against the G4 timescale (Petit *et al*., 1999, 1997) at Taylor Dome (Steig *et al*., 1999, 1998) with the accurate st9810 timescale only, at Byrd (Beer *et al*., 1987) with its original timescale, as well as the ^{10}Be concentration data from 719–2253 m at GISP2 Greenland station (Finkel *et al*., 1997, Alley *et al*., 1995, Davis *et al*., 1990). A different element used for a check is the Mg ions from Taylor Dome (Stager *et al*., 1997, Mayewski *et al*., 1996, Steig *et al*., 1999).

As would be the case with all the time scales used for the same data, the LaViolette (1983) time scale has varied reliability, too. I later modify that scale (with the relative ^{10}Be production rate normalized to the Holocene average value) by boosting no peaks in data, contrary to what many researchers do using solar screening models to correct for solar screening effects during the Holocene period of enhanced solar activity. Another way of determining what the relative cosmic ray intensities would be outside the solar system is as follows: perform a data separation on raw data, rather than editing the data or restricting the analysis to the interval when the peaks are high such as during the ice age periods but excluding the interglacial. Namely, one can never understand inherently gapped data or portions of such data so well as to be assured that data alterations used to correct known issues would not introduce a slew of new (unknown) issues. Analogously, no other parts of the time series were adjusted for solar screening, not even during interstadial intervals, since there is a lack of data to apply a model. Going along the reference timescale used, the coral chronology developed by Bard *et al*. (2004, 1990) allows corrections as far back as about 20–30 kyr, but for earlier dates, there is no reliable way how to correct the ^{14}C values since there

https://doi/org/10.5281/zenodo.5228497

are no dendrochronology or carved sediment scales available to go by for times beyond about 20 kyr (a conservative estimate). Dates from about 20–70 kyr BP were based on ^{14}C but are not as reliable as the earlier ice core dates due to an unknown amount by which ^{14}C dates ought to be adjusted. The ice core dates from about 70 kyr to 14 kyr BP are based on K/Ar dates and therefore are considered the least reliable in the record. An alternative timescale, which was an update of the LaViolette (1983) scale based on findings by Henderson and Slowey (2000), was also tried in the end. However, that timescale returned non-converging results.

Value #	t_i [years BP]	^{10}Be $\left[\frac{\text{atoms}}{\text{cm}^2 \cdot \text{year}} 10^{-5}\right]$	Value #	t_i [years BP]	^{10}Be $\left[\frac{\text{atoms}}{\text{cm}^2 \cdot \text{year}} 10^{-5}\right]$	Value #	t_i [years BP]	^{10}Be $\left[\frac{\text{atoms}}{\text{cm}^2 \cdot \text{year}} 10^{-5}\right]$
001	00.00	**2.45**	045	14.02	**2.46**	089	67.92	**2.66**
002	00.43	1.96	046	14.39	**2.44**	090	70.00	**3.84**
003	01.12	1.63	047	15.23	**2.09**	091	71.75	**2.31**
004	01.26	1.68	048	15.49	1.58	092	73.50	**2.63**
005	01.50	1.92	049	15.52	1.72	093	75.24	**2.08**
006	02.30	1.83	050	15.85	**2.14**	094	76.99	1.86
007	02.57	1.52	051	16.67	1.93	095	78.74	1.98
008	02.92	1.50	052	17.34	**2.16**	096	80.49	**2.24**
009	02.93	1.41	053	17.53	**2.72**	097	82.24	**2.75**
010	03.35	1.48	054	18.36	**2.20**	098	83.99	**2.51**
011	04.16	1.68	055	18.58	**2.49**	099	85.73	**2.61**
012	04.41	1.37	056	19.23	**2.67**	100	87.48	**2.43**
013	04.42	1.88	057	19.49	1.93	101	89.23	**3.22**
014	04.72	**2.01**	058	21.13	**2.53**	102	90.98	**3.18**
015	05.06	1.61	059	23.02	**2.88**	103	92.73	**2.75**
016	05.34	**2.78**	060	24.92	**2.38**	104	94.48	**2.67**
017	05.73	1.90	061	26.81	**2.86**	105	96.22	**2.16**
018	05.79	1.72	062	28.70	1.97	106	97.97	**2.43**
019	06.03	1.94	063	30.60	**2.26**	107	99.72	**2.90**
020	06.28	**2.10**	064	32.35	**2.87**	108	101.47	1.80
021	06.76	1.66	065	33.55	**3.09**	109	103.22	**3.41**
022	06.86	1.85	066	34.11	**4.70**	110	104.97	**2.75**
023	07.27	1.94	067	34.68	**4.10**	111	106.71	**2.33**
024	07.61	1.54	068	35.66	**3.81**	112	108.46	**2.31**
025	07.79	1.37	069	35.94	**2.53**	113	110.35	**2.93**
026	07.94	**2.10**	070	36.58	**2.87**	114	112.08	1.78
027	08.49	1.81	071	37.63	**3.09**	115	113.82	1.69
028	08.69	1.74	072	39.64	1.78	116	115.56	1.78
029	09.01	1.32	073	41.69	1.81	117	117.29	1.69
030	09.20	1.39	074	43.74	**2.05**	118	119.03	1.64
031	09.69	1.43	075	45.79	1.66	119	120.76	1.78
032	09.96	1.83	076	47.84	**2.04**	120	122.50	1.44
033	10.08	1.90	077	49.89	**2.07**	121	124.22	1.92
034	10.49	1.57	078	51.93	**2.21**	122	125.95	1.44
035	10.92	1.74	079	53.98	**2.07**	123	127.67	**2.20**
036	11.16	**2.05**	080	55.98	1.80	124	129.54	**2.82**
037	11.21	**2.45**	081	57.97	**2.25**	125	131.46	**4.26**
038	11.35	**2.36**	082	59.16	**3.09**	126	133.60	**2.49**
039	11.43	**2.98**	083	59.95	**4.02**	127	136.61	1.97
040	12.30	1.77	084	60.75	**2.86**	128	139.63	1.92
041	12.70	1.49	085	61.14	**2.69**	129	142.64	1.64
042	13.15	1.45	086	61.94	**2.08**	130	145.65	**2.00**
043	13.37	**2.00**	087	63.92	**2.21**	131	148.66	1.64
044	13.95	1.94	088	65.90	**2.56**	131	148.66	1.64

Table 1. Vostok ^{10}Be deposition rate raw data (Raisbeck *et al*., 1987, 1992), LaViolette (1983) timescale. Values at-and-above $2{\cdot}10^5$ atoms/cm²/yr cutoff marked in boldface.

https://doi/org/10.5281/zenodo.5228497

A real-life situation in which researchers must rely on timescales like described above is something that researchers face daily and is indicative of what I warned about in the Introduction when I argued that new approaches to climatic data analysis are needed altogether: spectral analyses of severely altered yet poorly understood records are highly questionable. Thus given the time-span and density, I only consider the 99%-confidence level estimates. To obtain the ^{10}Be deposition rate data, I lastly adjust the ^{10}Be ice concentrations for the ice accumulation rate tied in with the ice core assumed chronology (LaViolette, personal communication 2006). Still, using the spectral analysis based on a least-squares fit, I demonstrate that timescales are not the primary issue of concern in climate studies. Climate researchers should instead focus their efforts on the data of interest and especially on data treatment.

3. Spectral analysis

The raw ^{10}Be data were analyzed using the Gauss-Vaníček Spectral Analysis (Vaníček, 1969, 1971) that fits in the least-squares sense data with trigonometric functions. Magnitudes of GVSA spectrum peaks depict the contribution of a period to the variance of the time-series, of the order of % (Vaníček, 1969). As a result, and based on the variance as the most direct measure of noise, the G-V spectra generally depict background noise levels linearly, which gives the GVSA a physical meaning, making it a preferred technique for studying processes and fields simultaneously (Omerbashich, 2006).

In addition, periodicity from incomplete records is estimated down to accuracy prescribed by data, i.e., to the last reliable digit of data values, so that only general reliability (precision) of the input data gets superimposed onto the G-V spectrum. At the same time, the method precision depends solely on the spectral resolution that can be freely set. Given its character as a general optimizer, a least-squares fit will outperform the labeled reliability of data it fits most of the time by as much as 90%.

The accompanying statistical analysis in GVSA is both intuitive and straightforward, while computer execution time is a non-issue, with little preprocessing and no post-processing required. The GVSA has been in use in astronomy, geophysics, medicine, finances, and other disciplines. Taylor and Hamilton (1972) and Omerbashich (2003) report (blind) performance tests. The GVSA outperforms Fourier spectral analysis when studying long periods in long records of natural data (Press *et al.*, 2003; Omerbashich, 2006), such as the data used here. Subsequently, the method saw simplifications into non-rigorous (strictly non-least-squares) formats, such as the Lomb-Scargle technique. GVSA provides total (absolute) accuracy in extracting periods from natural data sets — to the prescribed accuracy of analyzed data themselves (Omerbashich, 2007; 2021).

A peak in the G-V spectrum is well-resolved when resolved from both sides (slopes); meaning if a spectrum ascends immediately (i.e., in a nearly straightforward fashion) from zero to the maximum (the spectral peak) and without retaining its maximum for longer than one spectral point continues to descend in the same manner towards zero. The accuracy of the period's least-squares estimate of a well-resolved peak is obtained uniformly for the entire dataset; it equals the declared accuracy of input data, taken over the data density (as data time-span over the number of data input values). Note that any labeled uncertainties in the G-V periods' estimates must not be taken at their face value, as raw data are noise-contaminated. Thus, realistically, estimate uncertainties could reach up to several times greater values than what is labeled, but this is empirical.

As seen from Fig. 3, the G-V period estimates converge rapidly with a magnitude-of-order increase in spectral resolution. Since computations with spectral resolution on the order of $2 \cdot 10^5$ spectral points can be burdensome on computing capabilities, I subsequently use $2 \cdot 10^4$ points resolution throughout. Note here that the estimate precision stays on the order of (some) years when going from $2 \cdot 10^4$ to $2 \cdot 10^5$ points resolutions. Note that the Vostok data, Table 1, for the period between 0 and 19 kyr BP are sampled more densely with samples taken every 3-13 m; afterward, the sampling interval was every 25 m for the most part. However, one should not worry about the sample being denser towards its beginning, Table 1, given the scarcity of values over such a long span. Unless otherwise stated, the band of interest for this analysis is 400–40000 years.

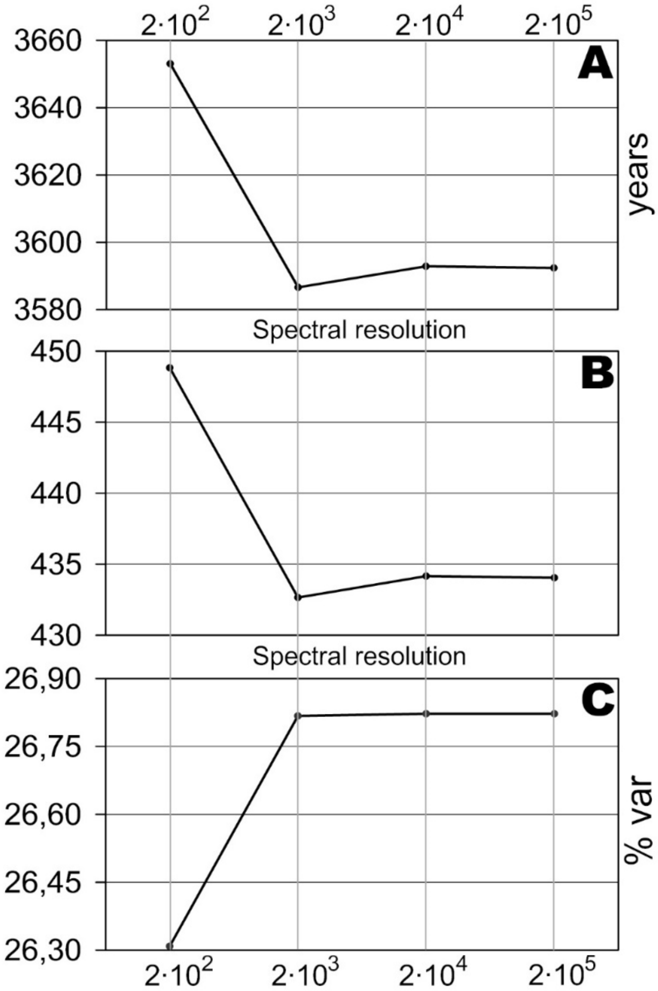

Figure 3. Convergence of GVSA strongest-period estimate with a magnitude-of-order increase in spectral resolution. From Vostok ^{10}Be raw data at 99% confidence level. Spectral resolution in integer number of spectral points (spectral lines). A: period estimate, B: estimate fidelity, C: period magnitude.

#	period [yr]	fidelity	mag (%var)	power (dB)
1	5583	1048	19.3	-6.2
2	3592	434	26.8	-4.4
3	2296	177	11.9	-8.7
4	1908	122	10.1	-9.5
5	1206	49	9.2	-9.9

Table 2. GVSA periods found in Vostok ^{10}Be deposition rate raw data, at 99% confidence level, Fig. 4. Data span: t = 148 663 yr. Number of input values: N = 131, Table 1. Data' declared precision: 95%. Period estimate uncertainty (uniform): $\Delta T = (t / N) \cdot 5\%$ = ±57 yr. Spectral resolution: $2 \cdot 10^5$ spectral points.

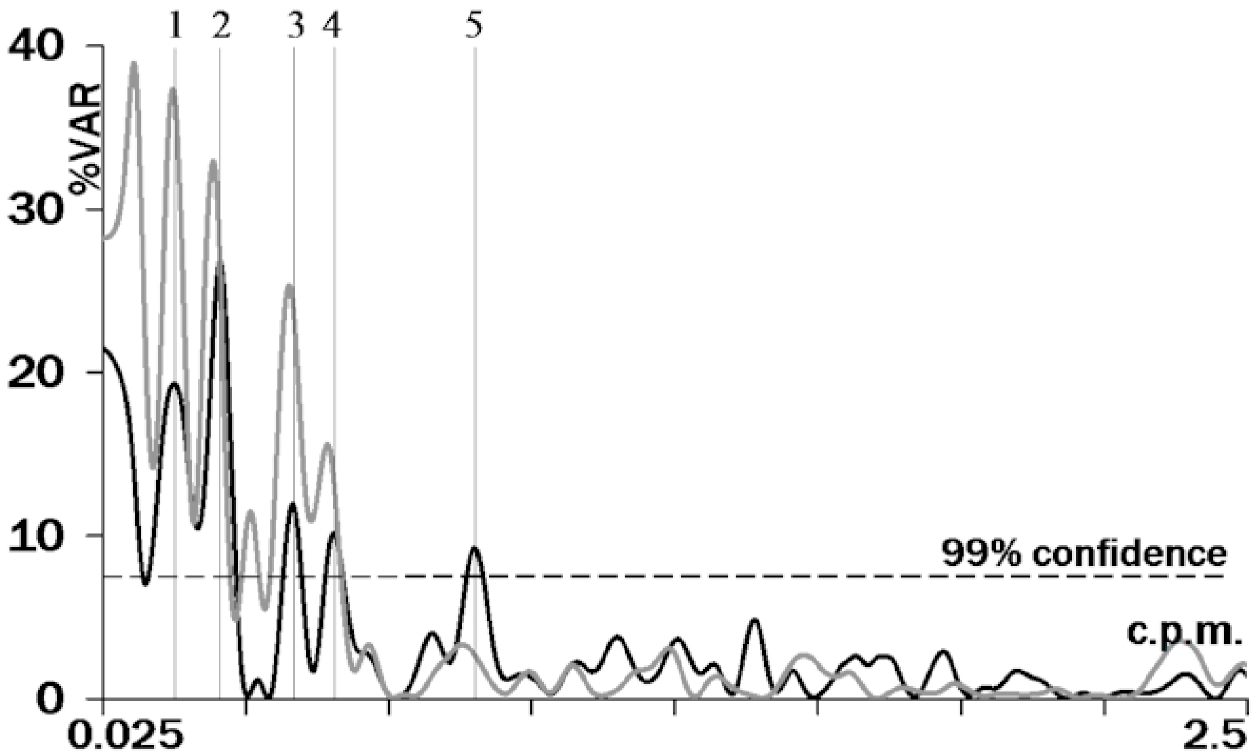

Figure 4. Gauss-Vaníček (G-V) spectrum of the ^{10}Be Vostok deposition rate raw data with LaViolette (1983) time-scale (black) v. G4 time-scale (gray). Corresponding periods' estimates #1-5 listed in Table 2. Frequency units in cycles per 1 kyr, or cycles per 1 millennium (c.p.m.).

The highest spectral peak detected in ^{10}Be deposition rate raw data is 3592±57 yr, Table 2. It was previously reported neither in ice core ^{10}Be analyses nor tree-ring radiocarbon analyses. However, Gogorza *et al*. (1999) have reported this period in geomagnetic field declinations. To the best of my knowledge, the periodicity estimate #3, of 2296±57 yr, could represent the best estimate of the Hallstadzeit solar cycle yet. The Hallstadzeit cycle has been reported previously with values ranging anywhere between 2000–2500 years, both in ice core ^{10}Be studies and in tree ring studies; see, e.g., approximate estimates by Tobias *et al*. (2004), Sonett (1990), and Sonett and Finney (1990). The above excellent estimate of this period is no coincidence since raw data were used (as the only criterion of validity) with an analysis method that can accommodate that norm in an optimal way (least-squares fit). Note Hallstadzeit cycle estimate worsens somewhat but not significantly when using the G4 scale; see Table 3. The period estimate #1, Table 2, has been reported previously also from the 150-kyr long Vostok ^{10}Be record, though as a coarse "5 kyr"; see Liritzis and Gregori (1997). No periods #4 and #5, Table 2, have been reported previously to the best of my knowledge. These could be related to the multi-century cooling episodes known to have occurred every 1500±500 yr during the Holocene; see a review by deMenocal (2001).

The Vostok ^{10}Be deposition rate raw data show no significant periods at 19000, 40000, or 100000 yr. LaViolette (1983, 1987) claimed that a ca. 12500 yr period would be the strongest in ^{10}Be data. There is some increase in the G-V spectrum of ^{10}Be deposition rate raw data at around 12500 yr, but it is too unclear and low to be called a period. Besides, given that the Vostok data span is only ~140 kyr, it makes no sense to claim anything longer than 1/4 of that, i.e., ~35 kyr. Here I discuss the strongest period found in the present study, at ca. 3600 yr.

https://doi/org/10.5281/zenodo.5228497

#	period [yr]	fidelity	mag (%var)	power (dB)
1	12427	5115	38.9	-1.9
2	6060	1216	37.4	-2.2
3	3950	517	32.9	-3.1
4	2993	297	11.5	-8.9
5	2390	189	25.3	-4.7
6	1995	132	15.6	-7.3

Table 3. GVSA periods found in Vostok ^{10}Be deposition rate raw data, at 99% confidence level, Fig. 5. Data span: t = 150 972 yr. Number of input values: N = 131, Table 1. Data' declared precision: 95%. Period estimate uncertainty (uniform): $\Delta T = (t / N) \cdot 5\%$ = ±58 yr. Spectral resolution: $2 \cdot 10^4$ spectral points. G4 timescale.

Peaks in the G-V spectrum of Vostok data on the G4 timescale appear well resolved from both sides and very sharp, with underlying background noise suppressed, Fig. 4. However, the impression is that the creators of the G4 timescale were worried more about details but missed the big picture. The 12500 yr period appearance is most likely due to precession modulation. Note deterioration in the estimate of the Hallstadzeit cycle from the data on the G4 timescale.

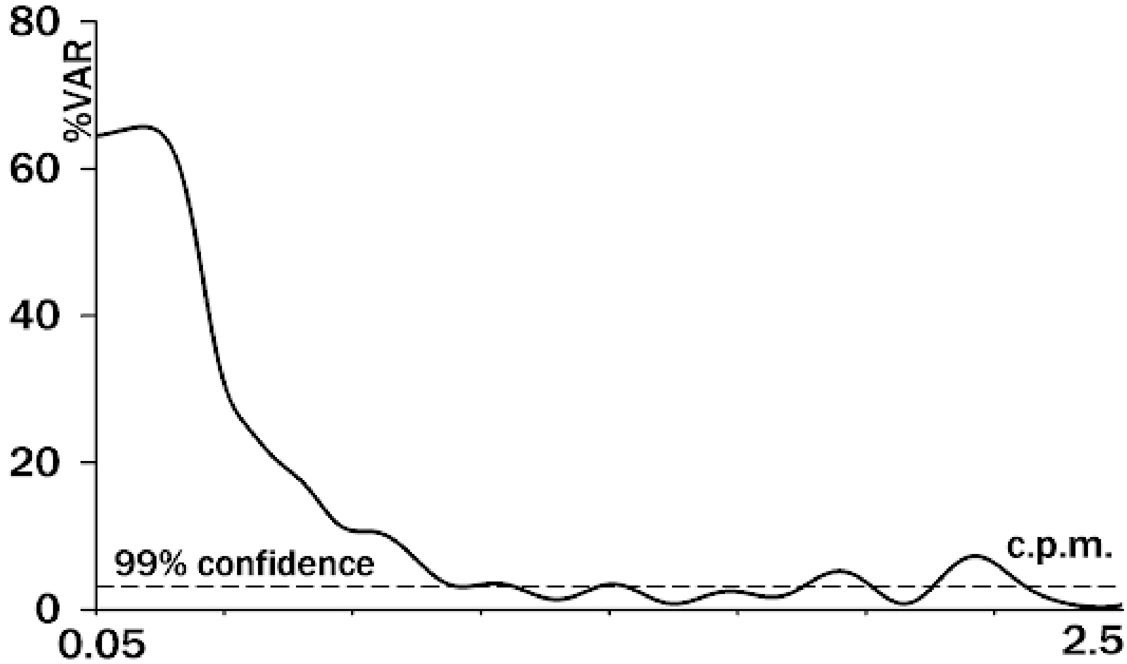

Figure 5. G-V spectrum of GISP2 Greenland record of ^{10}Be concentration raw data.

The ^{10}Be raw data from ice cores at Greenland show no significant peaks as long-periodic noise burdens the raw data, Fig. 5, perhaps due to a higher snowfall rate than in Antarctica or significant climate variability on sub millennium scales. However, climate variability in Greenland v. Antarctica does not appear to significantly differ on millennium to decadal scales (Mayewski *et al*., 1996). The first reliable studies on Greenland-Antarctica snowfall and other glacial variability were by the ITASE project (Mayewski and Goodwin, 1996). In addition, a southerly-directional influx of extreme cosmic radiation could have further helped make natural periods remain buried inside the extremal levels of long-periodic noise in the Greenland record.

Beer *et al*. (1987) did not analyze the Holocene part of the Byrd ice core. Their data begins at around 9200 yr BP. No sensible results could be obtained in the present study using those data.

#	period [yr]	fidelity	mag (%var)	power (dB)
1	18448	7544	25.9	-4.6
2	10846	2608	28.2	-4.1
3	4305	411	21.5	-5.6
4	3825	324	21.5	-5.6
5	2251	112	28.7	-3.9
6	1701	64	5.6	-12.2

Table 4. GVSA periods found in Taylor Dome ^{10}Be concentration raw data, at 99% confidence level. Data span: t = 225600 yr. Number of input values: N = 185. Data' declared precision: 95%. Period estimate uncertainty (uniform): $\Delta T = (t / N) \cdot 5\% = \pm 61$ yr. Spectral resolution: $2 \cdot 10^4$ spectral points. 'st9810' timescale.

#	period [yr]	fidelity	mag (%var)	power (dB)
1	5503	4657	28.7	-3.9
2	1570	379	46.8	-0.6
3	950	139	19.5	-6.2

Table 5. GVSA periods found in Byrd ^{10}Be concentration raw data, at 99% confidence level. Data span: t = 32 510 yr. Number of input values: N = 73. Data' assumed precision: 80%. Period estimate uncertainty (uniform): $\Delta T = (t / N) \cdot 20\% = \pm 89$ yr. Spectral resolution: $2 \cdot 10^4$ spectral points. Original timescale.

The ^{10}Be concentration raw data reveal no periods longer than 5503 yr, and there is no ~3600 yr period. Empirically, GVSA can discern a period if the total data span is at least four to eight times the same period under ideal conditions (noise absent). However, the variance-contribution mostly was absorbed by the detected widely spread 40-kyr period (under 99% confidence), so this empirical requirement does not necessarily apply. The 40-kyr period here is recognized as the 39200-yr obliquity, cf. the Berger's equations (Berger and Loutre, 1992). Enforcing the 39200 yr period in the Vostok data lowers the strength of all the periods considerably. However, the span is too short for the data to reflect such a long period.

As seen from Tables 2 and 6, the estimate of the discovered period picks strength from using concentrations rather than deposition rates. However, in addition to the spectral peak's magnitude increase, the underlying long-periodic noise doubles as well, so that this magnitude gain seen in the strongest period is only apparent. What matters the most is that, in both cases, the periods' extraction occurred at or above the 99% confidence level. As variance measures classical noise, so does %var measure the signal, as imprinted in the noise rather than signal. Whether a signal from one dataset comes out stronger in GVSA than from another dataset, where both are above 99% confidence level, has little to do with data values themselves but more with either the data sensitivity to noise or the level and type of noise pollution (reliability).

Therefore, compared to the Taylor ^{10}Be concentration raw data, representing the ^{10}Be raw data as concentrations rather than deposition rates does not affect the accuracy of the period estimate. While the 99% confidence level remained about the same 7.5%var, the signal doubled (i.e., noise halved), bringing the period to the 30-40%var range, while the Taylor signal is in 20-30%var range. However, at the same time, thanks to the GVSA-unique linear representation of background noise (Omerbashich, 2006), it is discernable that the underlying noise doubled in magnitude, as well.

https://doi/org/10.5281/zenodo.5228497

#	period [yr]	fidelity	mag (%var)	power (dB)
1	12563	5304	44.4	-1.0
2	5926	1181	30.3	-3.6
3	3721	466	38.7	-2.0
4	2291	176	18.1	-6.6
5	1935	126	12.5	-8.5

Table 6. GVSA periods found in Vostok ^{10}Be concentration raw data, at 99% confidence level. Data span: t = 148 663 yr. Number of input values: N = 131. Data' assumed precision: 95%. Period estimate uncertainty (uniform): $\Delta T = (t / N) \cdot 5\% = \pm 57$ yr. Spectral resolution: $2 \cdot 10^4$ spectral points.

As a minimum, it should come expected (see section 2) that the Vostok ^{10}Be data are not less reliable than Taylor Dome data; although the periods did double, they still are not any better resolved. Quite contrary: there seems to be a background process seen as the degree of unresolved range of periods, in %var, i.e., from 0%var to some %var, that goes up in the same manner as the longest-periodic portion of the band of the drawn periods does. So much so that it appears to be the different data representation rather than accuracy that affects the signal-to-noise ratio. In other words, the doubling of the S-N ratio is artificial – meaning due to data processing and not the data per se. Finally, peaks in a G-V spectrum follow the Boltzmann distribution (Steeves, 1981), so that any change in data representation could perhaps introduce some Boltzmann-distributed noise as well.

At the same time, it appears reasonable to expect that the ^{10}Be concentration data should reflect not only the 3600-yr sensitivity of ^{10}Be but of other information contents as well since it mostly is simple additions of noise effects that occur when using concentrations (meaning, the noise sensitivity adds up uniformly). Deposition rates, on the other hand, by definition imply the rates of change of ^{10}Be only so that the effects of most of the other contents arithmetically cancel out. Thus, representing ^{10}Be data in terms of deposition rates acts as a band-pass filter, lowering (or halving, as in this case) the impact of any concentration magnification. Finally, by definition, ^{10}Be concentration raw data do not reflect the changes in ice accumulation rate. Climatic variations that cause sudden spikes in the ice accumulation rate can also introduce outliers in data or even shift concentration maxima.

The spectra of cosmic-ray proton background radiations (LaViolette, 1983; Fig. 3.7, p.72) show the current electron spectrum and the current proton spectrum, both at solar minimum. The electron cosmic-ray energy density is about 1% that of the proton cosmic-rays, which for protons is $3 \cdot 10^{-2}$ ergs/cm^2/s (Ramaty, 1974; Fig. III-15). The other 99% is the cosmic ray proton background, which is mostly of extragalactic origin in that it is distributed isotropically. These are the particles emitted from explosive activity that long ago took place in other galaxies. Thus the marker ^{10}Be deposition rates that prevail during the Holocene interval of about 0 to 10 kyr BP and the previous Eemian interglacial would reflect times when the background was almost entirely of extragalactic origin. Small (weaker) waves might be present but would get lost in the background noise. Since cosmic-ray electrons are much less efficient producers of ^{10}Be, and since it is believed there exists a significant solar-screening effect by the heliopause sheath, the cosmic-ray burst wave component might have to raise almost 10^5 fold before it would be possible even to see it above the extragalactic proton background signal. Subsequently, LaViolette (1983) proposed that a Galactic burst wave exists so energetic as to be able to rise to a peak of $3 \cdot 10^5$ times the current cosmic-ray electron background, hence to 90 ergs/cm^2/s, as well as (p.233) that this wave peak electron intensity would have risen to 75 times the current cosmic-ray proton background (after taking into account solar modulation). So, during quiescent times when the burst wave cosmic-ray electron intensity was less than the current cosmic-ray proton background, the extragalactic proton background would have been the principal cause of the ^{10}Be production.

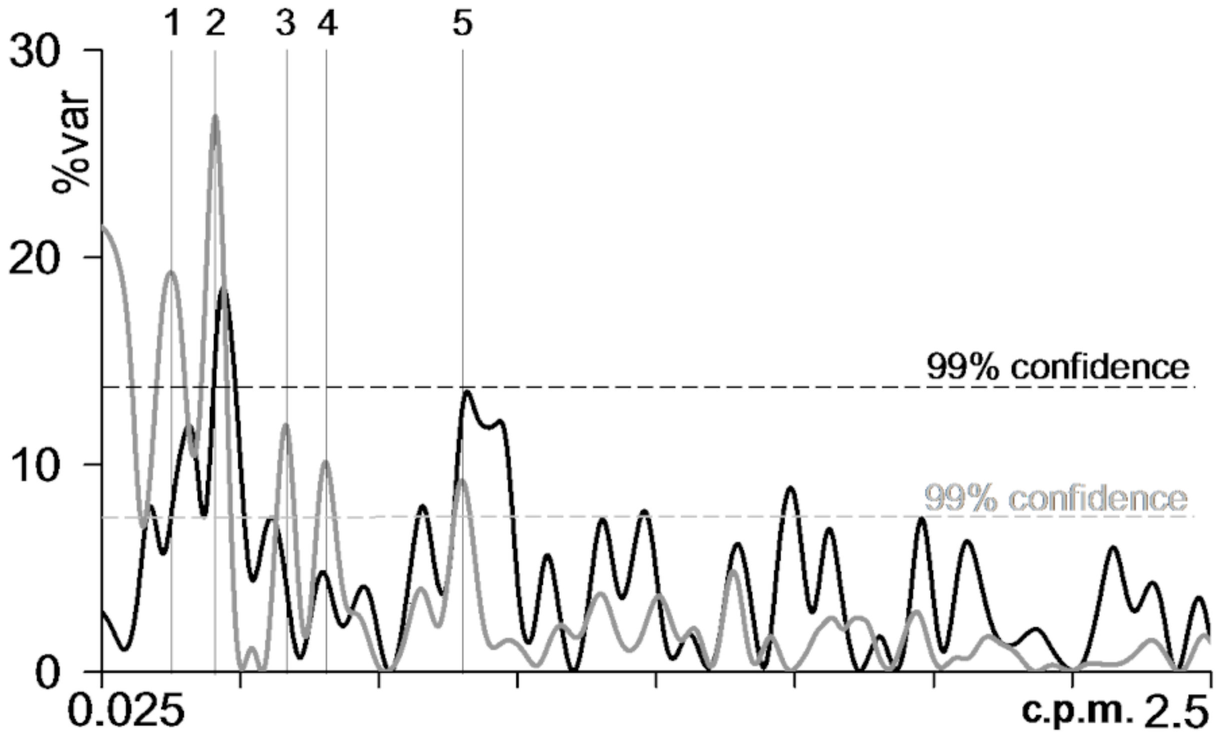

Figure 5. G-V spectra of Vostok ^{10}Be deposition rate raw data – all values in Table 1 (gray) v. Vostok ^{10}Be deposition rate raw at-and-above-cutoff data – boldface values in Table 1 (black). Periods' estimates 1-5 listed in Table 2.

Since I regard the use of raw data as *the* criterion for the validity of a physical result, I stay away from "correcting" (altering, actually) data for solar screening. Instead, I apply a data separation at the cutoffs of $2 \cdot 10^5$ atoms/cm^2/yr (for deposition rate) and $0.95 \cdot 10^5$ atoms/g of ice (for concentration dataset), which should reflect cosmic-ray background conditions at the Galactic boundary during the quiescent times (LaViolette, 1983). Thus, the cutoff values were selected such that most of the Holocene values remain below the threshold. At the same time, the chosen threshold excludes most of the data points from the low cosmic-ray intensity period during the previous interglacial.

The GVSA revealed that only the discovered period remains in the raw at-and-above-cutoff deposition rate and concentration ^{10}Be raw data, as 3378 ± 10^3 yr at 19% var, and 3346 ± 85 yr at 25% var (simple mean value 3362 yr), respectively. At the same time, the Hallstadzeit Solar cycle vanishes in both cases (datasets), which contradicts reports such as Tobias *et al*. (2004), who cite the Hallstadzeit period finding in the ice-ages portion of the GRIP ice core. Since the Hallstadzeit period vanishes after the separation in the deposition rate and concentration ^{10}Be raw data, there truly is a considerable sturdiness and purity associated with the 3400-yr (overall averaged at ~3600-yr) as the highest spectral peak found. Therefore I conclude that the newly discovered period is genuine. Moreover, it follows from the same observation on the decoupling of the two periods after data separation, that the source of the ~3600-yr period is: (a) extrasolar, because there exists any physically meaningful cutoff value which separates the ca. ~3600-yr and ca. 2300-yr periods, and (b) Galactic, because the selected cutoff value at the same time reflects the background conditions at the Galactic boundary.

If the Hallstadzeit cycle indeed does not appear in the ice-ages portion of the cores, this might indicate it as more important during periods of GC quiescence as during the Holocene when the solar cycle would be modulating a relatively constant galactic cosmic ray background (except for the spike around 5300 yr BP, if genuine). During the ice-age period when the GC was more active, the extrasolar cosmic-ray activity may have been so intense as to be able to drown out or overpower this subtle solar modulation cycle.

#	period [yr]	fidelity	mag (%var)	power (dB)
1	3378	392	18.5	-6.4

Table 7. GVSA periods found in Vostok ^{10}Be deposition rate raw data after separation at $2 \cdot 10^5$ atoms/cm^2/yr, at 95% confidence level. Data span: t = 145 651 yr. Number of input values: N = 71. Data' assumed precision: 95%. Period estimate uncertainty (uniform): ΔT = (t / N) · 5% = ±103 yr. Spectral resolution: $2 \cdot 10^4$ spectral points.

#	period [yr]	fidelity	mag (%var)	power (dB)
1	13246	5902	22.3	-5.4
2	7953	2127	23.8	-5.1
3	4428	659	16.7	-7.0
4	3346	376	25.2	-4.7
5	1651	92	11.8	-8.8
6	1359	62	14.3	-7.8
7	831	23	15.8	-7.3

Table 8. GVSA periods found in Vostok ^{10}Be concentration raw data after separation at $0.95 \cdot 10^5$ atoms/gram of ice, at 95% confidence level. Data span: t = 148 663 yr. No. of input values: N = 87. Data' assumed precision: 95%. Period estimate uncertainty (uniform): ΔT = (t / N) · 5% = ±85 yr. Spectral resolution: $2 \cdot 10^4$ spectral points.

#	period [yr]	fidelity	mag (%var)	power (dB)
1	11694	2973	39.3	-1.9
2	3965	342	43.6	-1.1
3	2464	132	35.0	-2.7
4	1698	63	11.6	-8.8

Table 9. GVSA periods found in Taylor Dome Mg concentration raw data. Data span: t = 229970 yr. Number of input values: N = 2969. Data' assumed precision: 80%. Period estimate uncertainty (uniform): ΔT = (t / N) · 20% = ±16 yr. Spectral resolution: $2 \cdot 10^4$ spectral points.

Note that lowering the confidence level would not bring much quality to the analysis in our case, as the only new "periods" that emerge in deposition rates at 95% are ~4500-yr, and one bulge (i.e., not even a defined period) at between 1100-1200 yr. Also, note that 131 deposition rate values were already a small number of points (after separation, that number went down to 71), so going anywhere below 99% does not make much sense. This data characteristic was the main reason why I opted for 99% as the minimum confidence level under these circumstances, i.e., given the kind of data, uncertain timescales, noise pollution, and for methodological reasons.

I next analyzed just the current quiescent period from 0–11,000 yr BP to see if the ~3600-yr period is absent. If the peak values of a galactic burst wave are, for the most part, below the background, and this period is related to the burst wave, then it should not be discernable during this more recent interval. The first 11 kyr of the Vostok ^{10}Be deposition rate raw data contains 35 values. GVSA of that portion in the 400-5500 yr spectral band reveals a 614-yr as the only period at 99% and no 95%-significant periods. On the other hand, after the data separation, the first 11 kyr of the at-and-above-cutoff raw Vostok data contains only five values. GVSA of that portion in the 400-5500 yr band reveals no significant period at either 99% or 95% confidence levels. There is a bulge at about 450-650 yr, but it can be declared a period only based on the above analysis of seven times denser data, not based on statistics as five is insufficient for the optimal number of input values in this case (although, strictly speaking, 3 is the minimum number of data values that GVSA can compute a spectrum from). Therefore, based on statistics and rather insufficient data, there is no ~3600 (~3400) -yr period in the last 11,000 yr of the Vostok recorded ^{10}Be chronology.

Finally, to check for possible effects of climatic variations, I analyze the magnesium data from Taylor Dome, Antarctica, as an indicator of crustal dust. These data should reflect climatic changes such as wind speed, continental dryness, and others, which affect the number of airborne dust particles. Results from the GVSA of Mg raw data from Taylor Dome are in Table 9. Note that, in addition to periods listed in Table 9 as the main ones to this study (like the 3965±16 yr period), many shorter periods were found also at the 99% confidence level and in the 400-114000 yr band; however, this was due to the 99% level itself dropping down to just 0.3% var. It appears that the Mg records are far more sensitive to short-term climatic disturbances than the ^{10}Be are. It can be seen from the analysis of the Mg data that the longest periods have the largest magnitudes, but also that they are "riding" on some unspecified background noise of up to 25 %var; this noise, however, was insufficient to bury them beyond recognition. This insight highlights the fact that one should not read magnitude strengths in the GVSA literally, but only in the context of the data analyzed and physical processes those data are (un)known to be sensitive to. This find is also related to what I have noted earlier: in absolute terms, the result that the magnitudes of longest periods from ^{10}Be concentration data appear twice the magnitudes from ^{10}Be deposition rate data does not mean this is the output one wants to use as an argument. On the contrary, it means that there are issues with the input data, but those issues are unimportant in that in both cases longest periods found exceeded the 99% confidence level.

Based on using GVSA and its raw-data single criterion, it seems as if timescales should not represent a big problem for climate studies, quite contrary to everyday understanding. If this is so, then most of the error budget in spectral analyses as applied to climate studies comes from the spectral analysis technique one uses. Namely, I seem to be finding my period in different kinds of records (^{10}Be, Mg) from geologically independent locations (Vostok, Taylor Dome), and regardless of timescale (except for Byrd, but where we have only 73 values with the datum not at zero but much later).

4. Epoch estimate

To estimate the epoch of the most recent increase in atmospheric ^{10}Be, I utilize a unique feature of GVSA: variance spectra depicting background noise levels linearly, enabling relative determination of field dynamics as shown by Omerbashich (2006). Furthermore, this feature allows relative measurement of the effect of dataset size on the periods' estimate, making the G-V spectrum an indirect gauge of signal's relative strength as the signal-to-noise ratio varies. Thus, one slides the data series for some random and small number of years (timestamps permit), say 350 yr in our case, then 869 yr, then 1224 yr, 254 yr, etc. If a period estimate increases at any of these values, despite the input dataset getting shortened, at that moment (datum), the so edited data are thus fit by the maximum number of cycles possible (maximal S-to-N ratio). In other words, the so shortened record is almost precisely at the beginning (datum) of a whole dominant cycle. The above procedure is repeated as many times as it makes sense physically - until the record gets shortened and the contribution of that period to variance (as found in the original dataset) extinguished. Then one can average so obtained estimates of the highest spectral peak in data, i.e., the estimates obtained when the period was increasing despite the data shortening.

https://doi/org/10.5281/zenodo.5228497

This procedure gives better results the higher the data density. In our case, this means proceeding with more than two dominant cycles back in the past to make three matches. Simple averaging of these three values yields an estimate of the last epoch of increased ^{10}Be on Earth, as 1085±57 CE. The results of the epoch estimate are summarized in Table 10. The described procedure can be laborious, so selecting datum shifts should be performed in a fashion as random as possible; the likelihood of obtaining an estimate of the last-occurred epoch drops suddenly if systematic datum-shifting is employed instead, see Table 11.

shift #	T_i @99%conf [yr]	$\Delta T_i = T_{i+1} - T_i$ [yr]	mag_i [%var]	fidelity	N_i	$(N_o - N_i) < (N_o \times mag_o)$	1/dens= span/N [yr]	datum $shift_i$ [yr]	$b_i = shift_i - shift_{i+1}$ [yr BP]	epoch = b_i + 1950 [yr CE]
0 (raw)	**(3592.7)**	**+0.9**	**(26.8)**	**(434.0)**	**131**	**yes**	**(1135)**	**(427.0)**	**-697.4**	**1253**
1	3593.6	-5.0	26.8	435.6	130	yes	1140	1124.5	-375.5	
2	3588.6	-17.0	26.9	436.4	129	yes	1144	1500.0	-796.1	
3	3571.6	-5.2	27.6	433.4	127	yes	1159	2296.1	-622.8	
4	3566.4	-15.4	27.7	434.5	126	yes	1162	2918.9	-430.9	
5	3550.9	-22.3	28.1	432.6	124	yes	1175	3349.8	-811.2	
6	3528.6	-11.1	28.8	428.4	122	yes	1191	4160.9	-557.9	
7	3517.5	-24.6	29.1	428.1	121	yes	1194	4718.9	-620.6	
8	3493.0	-12.1	29.6	423.8	118	yes	1220	5339.5	-385.8	
9	**3480.8**	**+8.9**	**29.7**	**422.7**	**116**	**yes**	**1236**	**5725.3**	**-1030.0**	**920**
10	3489.8	-14.8	30.0	426.0	115	yes	1243	6755.4	-512.4	
11	3475.0	-11.8	29.8	425.5	111	yes	1278	7267.8	-346.8	
12	3463.2	-2.5	29.5	424.1	109	yes	1297	7614.6	-323.2	
13	3460.6	-22.2	29.3	424.5	108	yes	1306	7937.8	-556.2	
14	3438.4	-0.3	28.9	420.1	106	yes	1328	8494.0	-516.7	
15	3438.1	-11.1	28.8	421.7	105	yes	1335	9010.7	-682.0	
16	3427.0	-29.5	28.2	420.5	103	yes	1356	9692.7	-391.0	
17	3397.5	-20.5	27.6	415.3	101	yes	1376	10083.7	-401.7	
18	3377.0	-5.4	26.9	411.4	99	yes	1400	10485.4	-431.3	
19	3371.6	-13.1	26.6	411.3	98	yes	1410	10916.7	-512.9	
20	**3358.5**	**+4.3**	**26.2**	**409.4**	**97**	**yes**	**1420**	**11429.6**	**-869.3**	**1081**
21	3362.8				93	no (STOP)				
									Average epoch CE:	**1085±57**

Table 10. Three estimates of the last epoch when the extreme level of ^{10}Be deposition rates occurred in the Vostok ice core raw data of N_0 values. Spectral resolution $2{\cdot}10^5$ pt throughout. First ΔT_i datum: 0.0 yr BP. Average epoch estimate from 3 locally non-negative (boldface) period changes caused by random datum shifts: 1085±57 CE. This is an example of a sufficient shift variability, resulting in three local increases in period estimate despite a reduced number of input values.

Counting back from the 1085 CE epoch, estimates for historical increases in the ^{10}Be level, Fig. 7, were obtained, where prediction of the coming maximum epoch fell in 4447 CE. Using the post-separation period's mean value of 3362 yr, Tables 7 & 8, the projected values are seen on Fig.7 as approximately matching some notable climate-altering events such as those reported by Jessen *et al*. (2005), as well as the related historical events. For instance, the 2227 BCE epoch matches the Akkadian (Mesopotamian) Empire sudden collapse in the late Holocene around 2220±150 BCE caused by extreme cooling (deMenocal, 2001) and the Old Egypt Kingdom sudden collapse around 2240 BCE caused partly by Sahara drying up due to global cooling (Street-Perrott *et al*., 2000). Then, the 1085 CE epoch matches the Tiwanaku (Bolivian-Peruvian) Empire collapse from around 1100 CE (deMenocal, 2001).

Finally, the 9001 BCE epoch matches the Late Pleistocene extinctions of thousands of species, including land-vertebrates such as most of the mammoth genus some 11000 years ago, where radiocarbon dating rejected most of the alternative theories on these extinctions (Guthrie, 2006), thus increasing plausibility for potential cosmic causes. Other matches may include the 19087 BCE estimate, coinciding with the beginning of the decline of the Wisconsin and Pinedale glacial maximums around 20000 years ago (Flannery, 1999). I note in the end that the initially predicted 1085 CE epoch, which matches seemingly well with the ancient Asian observation of a remarkable sky event, appears in terms of historical climate alterations as a match of the onset of the most extreme conditions of the Northern Hemisphere's Medieval Warm Period around 1000 CE (Cook *et al*., 2004, Kremenetski *et al*., 2004, Tiljander *et al*., 2003).

https://doi/org/10.5281/zenodo.5228497

shift #	T_i @99%conf [yr]	$\Delta T_i = T_{i+1} - T_i$ [yr]	mag_i [%var]	fidelity	N_i	$(N_o - N_i) < (N_o \times mag_o)$	1/dens= span/N [yr]	datum $shift_i$ [yr]	$b_i = shift_i - shift_{i+1}$ [yr BP]	epoch = b_i+ 1950 [yr CE]
0 (raw)	3825.7	-14.5	21.5	324,4	185	yes	(1219)	341.1	-310.2	
1	3811.2	-13.3	20.8	322.5	179	yes	1258	651.3	-266.0	
2	3797.9	-2.0	20.3	320.7	175	yes	1285	917.3	-291.0	
3	3795.9	-11.1	20.0	320.7	172	yes	1306	1208.3	-307.7	
4	3784.7	-20.4	19.6	319.2	169	yes	1328	1516.0	-351.9	
5	3764.5	-23.1	19.1	316.3	166	yes	1350	1867.9	-325.5	
6	3741.4	-14.4	18.7	312.9	163	yes	1372	2193.4	-365.9	
7	3727.0	-10.0	18.2	310.9	161	yes	1387	2559.3	-257.8	
8	3717.0	-2.8	17.6	309.8	158	yes	1411	2817.1	-259.2	
9	3714.2	-3.9	17.3	309.7	157	yes	1419	3076.3	-247.1	
10	3710.3	-3.2	16.8	309.4	155	yes	1435	3323.4	-310.9	
11	3707.1	-2.6	16.2	309.2	153	yes	1453	3634.3	-300.1	
12	3704.5	-2.7	15.7	309.2	151	yes	1470	3934.4	-309.6	
13	3701.8	-1.5	14.7	309.1	148	yes	1498	4244.0	-287.1	
14	3700.2	-0.7	14.1	309.3	146	yes	1516	4531.1	-386.1	
15	3699.6				144	no (STOP)				
									Average epoch CE:	**N/A**

Table 11. Three estimates of the last epoch when the extreme level of ^{10}Be concentrations occurred in the Taylor Dome ice core raw data of N_0 values. Spectral resolution $2 \cdot 10^5$ pt throughout. First ΔT_i datum: 31.5 yr BP. Average epoch estimate from locally non-negative period changes as caused by random datum shifts not possible. This is an example of insufficient datum-shift variability, resulting in no local increase in a period estimate (with reducing the number of input data values).

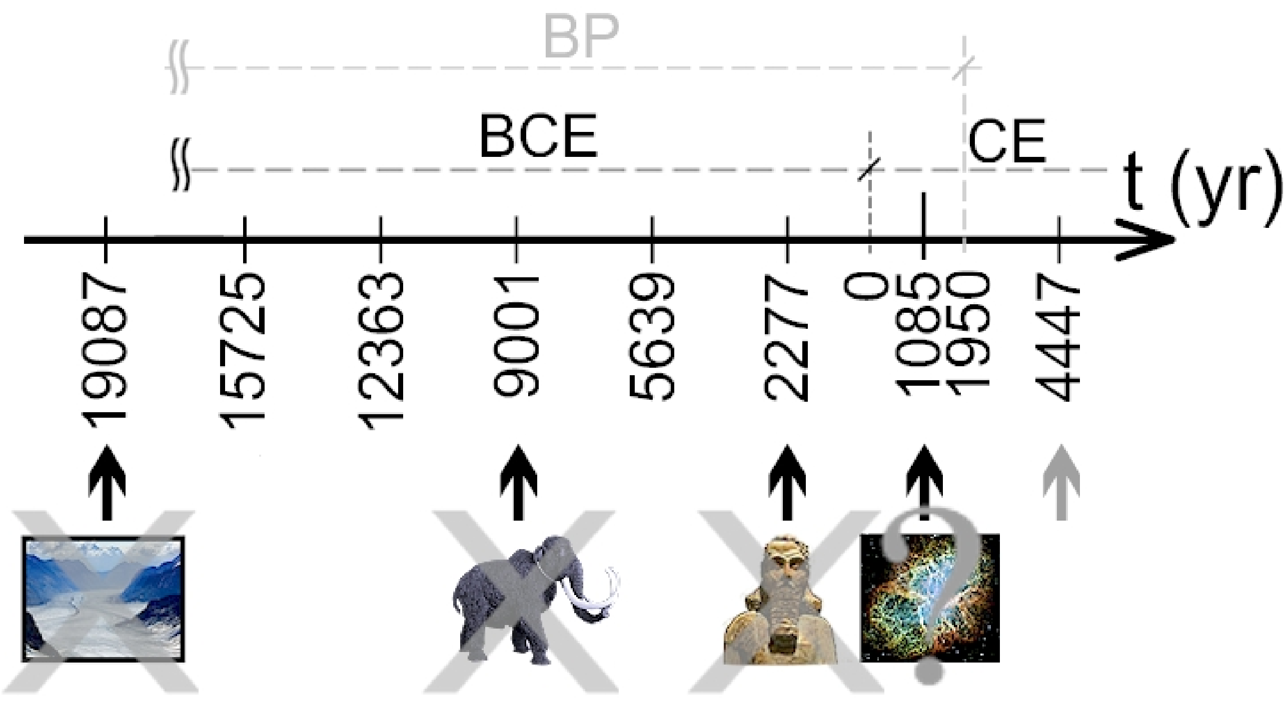

Figure 7. GVSA epoch estimates in years CE/BCE of the maximum levels of ^{10}Be on Earth. To get epochs of the real (atmospheric) maximums, subtract (add to BCE) some decades needed for significant ice accumulation of atmospheric isotope. Arrow markers indicate successful matches of the epoch estimate, Table 10, with known climate-related cultural collapses and mild (up to 50% of all genera variations) extinctions of species (black) and the epoch prediction of the next ^{10}Be maximum on Earth (gray).

https://doi/org/10.5281/zenodo.5228497

5. Discussion

According to Stephenson and Green (2005), some ten reliable eyewitness accounts of possible supernovae explosions have been identified on the record, covering the past two millennia. These records come from ancient Arab, Chinese, Japanese, Korean, North American natives, and other eastern and western sources. One of the most famous among such records is a Chinese historical account of a naked-eye observation of an extraordinary sky phenomenon that had taken place from 4–5 July 1054, dubbed “a guest star” by the ancient eyewitnesses. It lasted visibly for around 650 days at night, of which 23 days in the daylight also (Sollerman *et al*., 2001).

Some proposed that the event represented a supernova explosion, the SN1054 remnant of Crab nebula with its Crab pulsar in particular. The Crab nebula is one of the best-studied objects in the sky (*ibid*.). Not only is it the brightest optical remnant, but also marked by the most energetic pulsar in our galaxy. However, according to Peng-Yoke (1962), western knowledge or comprehension of the ancient Asian astronomical records appears quite limited. In addition, Peng-Yoke *et al*. (1972) have raised serious issues about the specific report of 1054, claiming that it did not mean observation of the Crab nebula at all. For instance, (*ibid*.) inspected an ancient Chinese text indicating that the “guest star” appeared as large as the Moon, which would by large exceed the usual angular size of any known supernovae. Also, Sollerman *et al*. (2001) have shown that the Crab supernova did not contain enough mass (Ni) to allow it to burn for almost two years.

Alternative explanations proposed by (*ibid*.) and earlier by Chevalier (1977) would require that, in the sense of mass-energy conversion modeling, the Crab nebula be unique in the entire Universe. I find this improbable. Beilicke *et al*. (2005) reported an unidentified extended TeV γ-ray source named HESS J1303-631 in the Southern Cross region close to the galactic plane. This report marked the second discovery of a TeV γ-ray source, following the confirmation on TEV J2032+4130 by Lang *et al*. (2005), which appears to mean a whole new class of galactic TeV γ-ray sources (Aharonian, 2005). Finally, H.E.S.S. telescope survey of the innermost 500 parsecs of the Galactic Centre region by Aharonian and coworkers (2006) observed very-high-energy γ-rays from the Galactic Centre ridge.

Furthermore, the number of galactic supernovae explosions described by historical accounts over the past millennium cannot be accounted for by galactic supernovae rates, e.g., Van Den Bergh (1991) and Donder and Vanbeveren (2003). Since it is unlikely that all of the unaccounted-for historic accounts meant naked-eye observations of extragalactic supernovae, alternative galactic explanations are needed instead for at least some of the above-mentioned historical accounts.

However, for lack of alternative reasoning that may explain the vast amounts of energy witnessed in 1054, many contemporary astronomers still refer to the 1054 event as the Crab nebula explosion. Besides the optical domain, the energy released from a supernova explosion significantly affects many other energy domains on Earth, as well; see, e.g., Iyudin (2002). Hence, authentic or not, the above historical references to supernovae explosions still set a threshold for this study. Specifically, since the energy released from a galactic supernova explosion leaves terrestrial signatures at atomic scales (*ibid*.), considerably higher energy emissions from past GC bursts could have affected the ^{10}Be records - so much that recurrence of such events reflected on all ice-core ^{10}Be data as the highest spectral peak overall. Such is the case with the ca. 3600-yr period discovered here.

6. Conclusions

Using raw data only, which also serves as the main criterion of a physical result's validity, I showed that many of the differing approaches to timescale definition for ice-core samples not only give erroneous results according to the criterion but are also hardly necessary at all. Namely, whatever ^{10}Be dataset or timescale one uses, the GVSA produces (or not) more or less the same periods, in most cases. This truth holds for elements other than Beryllium as well, such as Magnesium. Thus, using raw data as the most physical approach possible, remarkable features are revealed in the long-periodic (400–40000 yr) spectral band from most of the ^{10}Be ice-core raw datasets: they are strongly and clearly periodic with a previously unreported ca. ~3600-yr pulse, while at the same time the well-known Hallstadzeit Solar cycle was estimated likely to the highest degree of accuracy and confidence yet.

The timescale used here as the marker generally gave satisfactory results, such as one-on-one data separation v. results separation; the dominant period above 99% all the time regardless of the timescale or data density used; the pre-separation v. post-separation difference between two data representations seen as almost for an order of magnitude smaller than from the entire raw dataset; a curious match with significant climate-related historical events; and so on. That same timescale, when updated according to Henderson and Slowey (2000), produced distorted results such as seven new "periods" at 95% confidence level, with a complete mismatch between its 99%-periods in two data representations after separation, and no pre- v. post-separation convergence in the dominant period's estimate from two ways of data representation.

After data separation at the cutoffs reflecting cosmic-ray background conditions at the Galactic boundary, it emerged that the discovered period likely represents a signature of a recurrent LaViolette flare firing probably in the Galactic Center (GC) mid-half-kparsec region. A previously reported 3600-yr period in geomagnetic field declinations supports this conclusion on energy pulses sufficiently potent even for GC-Earth distances. Relying on Gauss-Vaniček spectral analysis-specific features, the epoch of the most recent ^{10}Be maximum on Earth was estimated, as ca. 1085. Given that it takes several decades for the ^{10}Be to accumulate in the ice differentially enough to presently detectable levels, this epoch falls remarkably close to the 1054–1056 CE historical account by Asian astronomers of an enormous sky explosion thought by some to represent the Crab supernovae explosion.

While Antarctica ice cores reveal ^{10}Be periodicity at a millennial recurrence rate, this signature could also represent a (previously confirmed or not) energetic-transient event from several my ago as it fades away in a quasiperiodic fashion. Alternatively, it could also mean the seeding of an arising such event.

Finally, I predicted by extrapolation the next maximum level of the ^{10}Be on Earth in 4463±57 CE. Should that happen, due to relatively prolonged exposure to significant energy rise and the exposure's relatively short recurrence period, recurring LaViolette galactic flares likely affect the Earth climate significantly and dramatically, albeit not necessarily forbiddingly for the overall survival of life.

Acknowledgments

The least-squares spectral analysis scientific software LSSA, based on the rigorous method by Vaníček (1969, 1971), was used to compute spectra. Dr. Spiros Pagiatakis (York University) provided LSSA v.5.0, now available from http://www2.unb.ca/gge/Research/GRL/LSSA/sourceCode.html. I thank Dr. Paul A. LaViolette for useful discussions and providing the Vostok original raw data sets and chronologies from his private collection.

Declarations

The author declares no competing interests.

References

Aharonian, F., Akhperjanian, A.G., Bazer-Bachi, A.R., Beilicke, M., Benbow, W., Berge, D., Bernlöhr, K., Boisson, C., Bolz, O., Borrel, V., Braun, I., Breitling, F., Brown, A.M., Chadwick, P.M., Chounet, L.-M., Cornils, R., Costamante, L., Degrange, B., Dickinson, H.J., Djannati-Ataï, A., 2006. Discovery of very-high-energy γ-rays from the Galactic Centre ridge. Nature 439, 7077, 695-698.

Aharonian, F., Akhperjanian, A.G., Aye, K.-M., Bazer-Bachi, A.R., Beilicke, M., Benbow, W., Berge, D., Berghaus, P.A., 2005. New population of very high energy gamma-ray sources in the Milky Way. Science 307, 5717, 1938-1942.

Aharonian, F., Akhperjanian, A.G., Aye, K.-M., Bazer-Bachi, A. R., Beilicke, M., Benbow, W., Berge, D., Berghaus, P., Bernlöhr, K., Bolz, O., Boisson, C., Borgmeier, C., Breitling, F., Brown, A.M., Bussons Gordo, J., Chadwick, P.M., Chitnis, V.R., Chounet, L.-M., Cornils, R., Costamante, L., 2004. High-energy particle acceleration in the shell of a supernova remnant. Nature 432, 7013, 75-77.

Alley, R.B., Finkel, R.C., Nishiizumi, K., Anandakrishnan, S., Shuman, C.A., Mershon, G.R., Zielinski, G.A., Mayewski, P.A., 1995. Changes in continental and sea-salt atmospheric loadings in central Greenland during the most recent deglaciation: Model-based estimates. J of Glaciology 41, 503-514.

Bard, E., Frank, M., 2006. Climate change and solar variability: What's new under the sun? Earth & Planetary Science Letters 248, 1/2, 480-493.

Bard, E., Ménot-Combes, G., Rostek, F., 2004. Present status of Radiocarbon calibration and comparison records based on Polynesian corals and Iberian Margin sediments. Radiocarbon 46, 1189-1203.

Bard, E., Raisbeck, G., Yiou, F., Jouzel, J., 2000. Solar irradiance during the last 1200 yr based on cosmogenic nuclides. Tellus B52, 985-992.

Bard, E., Hamelin, B., Fairbanks, R.G., Zindler, A., 1990. Calibration of the ^{14}C timescale over the past 30,000 years using mass spectrometric U-Th ages from Barbados corals. Nature 345, 405-410.

Beer, J., Blinov, A., Bonani, G., Finkel, R.C., Hofmann, H.J., Lehmann, B., Oeschger, H., Sigg, A., Schwander, J., Staffelbach, T., Stauffer, B., Suter, M., Wolfli, W., 1990. Use of ^{10}Be in polar ice to trace the 11-year cycle of solar activity. Nature 347, 6289, 164-166.

Beer, J. and coworkers, 1987. ^{10}Be measurements on polar ice: Comparison of Arctic and Antarctic records. Nuclear Instruments and Methods in Physics Research B29, 203–206.

Beilicke, M., Khelifi, B., Masterson, C., de Naurois, M., Raue, M., Rolland, L., Schlenker, S.,2005. Discovery of an unidentified TeV source in the field of view of PSR B1259-63 with H.E.S.S. AIP Conference Proceedings 745, 1, 347-352.

Benbow, W., 2005. The Status and Performance of H.E.S.S. AIP Conference Proceedings 745, 1, 611-616.
Benbow, W., 2006. The H.E.S.S. Experiment, AIP Conference Proceedings 842, 1, 998-1000.

Berger, A., Loutre, M.F., 1992. Stability of the astronomical frequencies over the Earth's history for paleoclimate studies. Science 255, 5044, 560-567.

Bélanger, G., Goldwurm, A., Renaud, M., Terrier, R., Melia, F., Lund, N., Paul, J., Skinner, G., Yusef-Zadeh, F.A., 2006. Persistent high-energy flux from the heart of the Milky Way: INTEGRAL's view of the Galactic Center. The Astrophysical Journal 636, 1, 275-289.

Bland-Hawthorn, J., Maloney, P.R., Sutherland, R., Groves, B., Guglielmo, B., Li, W., Curzons, A., Cecil, G., Fox, A.J. (2019) The Large-scale Ionization Cones in the Galaxy. The Astrophysical Journal 886:45-67.

Chevalier, R.A., 1977. Was SN1054 a Type II supernova? *Supernovae*, Ed. David N. Schramm. Astrophysics and Space Science Library 66, 53.

Cook, E.R., Esper, J., D'Arrigo, R.D., 2004. Extra-tropical Northern Hemisphere land temperature variability over the past 1000 years. Quaternary Science Reviews 23, 20-22, 2063-2074.

Davis, J.C., Proctor, I.D., Southon, J.R., Caffee, M.W., Heikkinen, D.W., Roberts, M.L., Moore, T.L., Turteltaub, K.W., Nelson, D.E., Loyd, D.H., Vogel, J.S., 1990. LLNL/UC AMS facility and research program. Nuclear Instruments and Methods in Physics Research B52, 269-272.

De Donder, E., Vanbeveren, D., 2003. The galactic evolution of the supernova rates. New Astronomy 8, 8, 817-837.
deMenocal, P.B., 2001. Cultural Responses to Climate Change During the Late Holocene. Science 292, 5517, 667-673.

Finkel, R.C., Nishiizumi, K., 1997. Beryllium 10 concentrations in the Greenland Ice Sheet Project 2 ice core from 3-40 ka. J of Geophysical Research 102, 26699-26706.

Flannery, T.F., 1999. Debating Extinction. Science 283, 5399, 182-184.

Gogorza, C.S.G., Sinito, A.M., di Tommaso, I., Vilas, J.F., Creer, K.M., Nuñez, H., 1999. Holocene geomagnetic secular variations recorded by sediments from Escondido Lake (south Argentina). Earth, Planets and Space 51, 93-106.

Guthrie, R.D., 2006. New carbon dates link climatic change with human colonization and Pleistocene extinctions. Nature 441, 7090, 207-209.

Hillas, A.M., 2005. Topical review: can diffusive shock acceleration in supernova remnants account for high-energy galactic cosmic rays? Journal of Physics G: Nuclear and Particle Physics 31, 5, R95-R131.

Henderson, G.M., Slowey, N.C., 2000. Evidence from U-Th dating against Northern Hemisphere forcing of the Penultimate glaciation. Nature 404, 61-66.

Hofmann, W., 2005. Status of ground-based gamma ray astronomy. AIP Conference Proceedings 745, 1, 246-259.
Iyudin, A.F., 2002. Terrestrial impact of the galactic historical SNe. J of Atmospheric and Solar-Terrestrial Physics 64, 5-6, 669-676.

Jessen, C.A., Rundgren, M., Björck, S., Hammarlund, D., 2005. Abrupt climatic changes and an unstable transition into a late Holocene Thermal Decline: a multiproxy lacustrine record from southern Sweden. Journal of Quaternary Science 20, 349-362.

Kremenetski, K.V., Boettger, T., MacDonald, G.M., Vaschalova, T., Sulerzhitsky, L., Hiller, A., 2004. Medieval climate warming and aridity as indicated by multiproxy evidence from the Kola Peninsula, Russia. Palaeogeography, Palaeoclimatology, Palaeoecology 209, 1-4, 113-125.

Lang, M.J., Carter-Lewis, D.A., Fegan, D.J., Fegan, S.J., Hillas, A.M., Lamb, R.C., Punch, M., Reynolds, P.T., Weekes, T.C., 2005. A New TeV Source Confirmed in Whipple Archival Data: TeV J2032+41. Astrophysics and Space Science 297, 1-4, 345-351.

LaViolette, P.A., 1983. Galactic explosions, cosmic dust invasions, and climatic change. Ph.D. dissertation, Portland State University, Portland, Oregon USA, 478 (763) pp.

LaViolette, P.A., 1987. Cosmic-ray volleys from the Galactic Center and their recent impact on the Earth environment. Earth Moon Planets 37, 241–286.

Liritzis, I., Gregori, K., 1997. Astronomical forcing in cosmogenic Be-10 variation from east Antarctica coast. Journal of Coastal Research 14, 3, 1065-1073.

Longair, M.S., 2002. High-energy astrophysics, in: Stars, the galaxy and the interstellar medium, Second edition, Cambridge University Press, Cambridge.

Mayewski, P.A., Twickler, M.S., Whitlow, S.I., Meeker, L.D., Yang, Q., Thomas, J., Kreutz, K., Grootes, P.M., Morse, D.L., Steig, E.J., Waddington, E.D., Saltzman, E., Whung, P.-Y., Taylor, K., 1996. Climate change during the last deglaciation in Antarctica. Science 272, 1636-1638.

Mayewski, P.A., Goodwin, I.D., 1996. Science and implementation plan. ITASE Workshop www2.umaine.edu/itase 2-3 August, Cambridge UK.

Monnin, E., Steig, E.J., Siegenthaler, U., Kawamura, K., Schwander, J., 2004. Stauffer, B., Stocker, T.F. Morse, D.L. Barnola, J.M. Bellier, B. Raynaud, D. Fischer, H. Evidence for substantial accumulation rate variability in Antarctica during the Holocene, through synchronization of CO_2 in the Taylor Dome, Dome C and DML ice cores. Earth and Planetary Science Letters 224, 45-54.

Morris, M. Serabyn, E., 1996. The Galactic Center environment. Annual Review of Astronomy & Astrophysics 34, 1, 645-57.

Muscheler, R., Joos, F., Müller, S.A., Snowball, I., 2005. How unusual is today's solar activity? (Arising from: S. K. Solanki, I.G. Usoskin, B. Kromer, M. Schüssler, J. Beer, Solanki *et al*., 2004. reply. Nature 431, 1084–1087). Nature 436, 7050, E3-E4.

Omerbashich, M., 2003. Earth-model Discrimination Method. PhD dissertation, Department of Geodesy and Geomatics Engineering, University of New Brunswick, Fredericton N.B., Canada, 129 pp.

Omerbashich, M., 2006. Gauss-Vaníček Spectral Analysis of the Sepkoski Compendium: No New Life Cycles. Computing in Science and Engineering 8, 4, 26-30. (Erratum due to journal error (2007) Comp. Sci. Eng. 9(4):5–6. DOI: https://doi.org/10.1109/MCSE.2007.79; full text: https://arxiv.org/abs/math-ph/0608014)

Omerbashich, M. (2007) Magnification of mantle resonance as a cause of tectonics. Geodinamica Acta 20(6):369-383.

Omerbashich, M. (2021) Non-marine tetrapod extinctions solve extinction periodicity mystery. Hist. Biol. 34 (29 March). https://doi.org/10.3166/ga.20.369-383

Peng-Yoke, H., 1962. Ancient and mediaeval observations of comets and novae in Chinese sources. Vistas in Astronomy , 127-225.

Peng-Yoke, H., Paar, F.W., Parsons, P.W., 1972. The Chinese guest star of CE 1054 and the Crab Nebula. Vistas in Astronomy 13, 1-13.

Petit, J.R., Jouzel, J., Raynaud, D., Barkov, N.I., Barnola, J.-M., Basile, I., Benders, M., Chappellaz, J., Davis, M., Delayque, G., Delmotte, M., Kotlyakov, V.M., Legrand, M., Lipenkov, V.Y., Lorius, C., Pépin, L., Ritz, C., Saltzman, E., Stievenard, M., 1999. Climate and atmospheric history of the past 420,000 years from the Vostok ice core. Antarctica, Nature 399, 429-436.

Petit, J.R., Basile, I., Leruyuet, A., Raynaud, D., Lorius, C., Jouzel, J., Stievenard, M., Lipenkov, V.Y., Barkov, N.I., Kudryashov, B.B., Davis, M., Saltzman, E., Kotlyakov, V., 1997. Four climate cycles in Vostok ice core. Nature 387, 359-360.

Press, W.H., Teukolsky, S.A., Vetterling, W.T., Flannery, B.P., 2003. Numerical Recipes. Cambridge University Press, Cambridge, United Kingdom.

Raisbeck, G.M. Yiou, F., 2004. Comment on ‘‘Millennium scale sunspot number reconstruction: Evidence for an unusually active Sun since the 1940s’’. Phys. Rev. Lett. 92, 19, 199-200.

Raisbeck, G.M., Yiou, F., Bourles, D., Lorius, C., Jouzel, J., Barkov, N.I., 1987. Evidence for two intervals of enhanced 10Be deposition in Antarctic ice during the last glacial period. Nature 326, 273-277.

Raisbeck, G.M., Yiou, F., Jouzel, J., Petit, J.R., Barkov, N.I., Bard, E., 1992. ^{10}Be deposition at Vostok, Antarctica during the last 50,000 years and its relationship to possible cosmogenic production variations during this period. In The Last Deglaciation: Absolute and Radiocarbon Chronologies (Proc. NATO ASI Series 12), edited by E. Bard and W. Broecker 127-140, Heidelberg: Springer-Verlag.

Ramaty, R., 1974. Cosmic Electrons, In: High Energy Particles and Quanta in Astrophysics. Edited by F.B. McDonald and C.E. Fichtel, Cambridge, Massachusetts, MIT Press.

Solanki, S.K., Usoskin, I.G., Kromer, B., Schüssler, M., Beer, J., 2004. An unusually active Sun during recent decades compared to the previous 11,000 years. Nature 431, 1084-1087.

Sollerman, J., Kozma, C., Lundqvist, P., 2001. Why did supernova 1054 shine at late times? Astronomy and Astrophysics 366, 197-201.

Sonett, C.P., 1990. Is the sun a long period variable? In: NASA, Goddard Space Flight Center, Climate Impact of Solar Variability, 106-114.

Sonett, C.P., Finney, S.A., 1990. The Spectrum of Radiocarbon, Philosophical Transactions of the Royal Society of London, Series A. Mathematical and Physical Sciences 330, 1615, 413-425.

Stager, J.C., Mayewski, P.A., 1997. Abrupt early to mid-Holocene climate transition registered at the equator and the poles. Science 276, 1834-1836.

Steeves, R.R., 1981. A statistical test for significance of peaks in the least squares spectrum. Collected papers of the Geodetic Survey, Department of Energy, Mines and Resources, Surveys and Mapping, Ottawa, Ontario Canada, 149-166.

Steig, E.J., Morse, D.L., Waddington, E.D., Stuiver, M., Grootes, P.M., 1999. Wisconsinan and Holocene climate history from an ice core at Taylor Dome, western Ross Embayment. Antarctica, Geografiska Annaler (in press).
Steig, E.J., Brook, E.J., White, J.W.C., Sucher, C.M., Bender, M.L., Lehman, S.J., Morse, D.L., Waddington, E.D., Clow, G.D., 1998. Synchronous climate changes in Antarctica and the North Atlantic. Science 282, 5386, 92-95.

Stephenson, F.R., Green, D.A., 2005. A Reappraisal of Some Proposed Historical Supernovae. J for the History of Astronomy 36, 2, 123, 217 - 229.

Street-Perrott, F.A., Holmes, J.A., Waller, M.P., Perrott, R.A., Allen, M.J., Barber, N.G.H., Fothergill, P.A., Harkness, D.D., Ivanovich, M., Kroon, D., 2000. Drought and dust deposition in the West African Sahel: a 5500-year record from Kajemarum Oasis, northeastern Nigeria. Holocene 10, 3, 293-302.

Taylor, J., Hamilton, S., 1972. Some tests of the Vaníček method of spectral analysis, Astroph. Space Sci, Int. J. Cosmic Phys. D.

Tiljander, M., Saarnisto, M., Ojala, A.E., Saarinen, T.A., 2003. 3000-year palaeoenvironmental record from annually laminated sediment of Lake Korttajärvi, central Finland. Boreas 32, 4, 566-577.

Tobias, S., Weiss, N., Beer, J., 2004. Long-term prediction of solar activity – a discussion… and a reply. Astronomy & Geophysics 45, 2, 6-7.

Usoskin, I.G., Solanki, S., Schuessler, M., Mursula, K., Alanko, K., 2003. A millennium scale sunspot number reconstruction: Evidence for an unusually active sun since the 1940's. Phys. Rev. Lett. 91, 21, 1101-1104.

Van Den Bergh, S., 1991. Supernova rates: A progress report. Physics Reports 204, 6, 385-400.

Vaníček, P., 1969. Approximate spectral analysis by least-squares fit. Astroph. Space Sci. 4, 387-391.

Vaníček, P., 1971. Further development and properties of the spectral analysis by least-squares fit. Astroph. Space Sci. 12, 10-33.